Full-Wave Characterization and CSRR Geometric Sensitivity Analysis of a Compact Slot-and-Ring-Loaded Multiband Microstrip Patch Antenna

Diksha Choudhary[1], Er. Satnam Singh[2]
[1,2]*Department of Electronics, SSCET Badhani Pathankot*

***Abstract*—This paper presents the full-wave design validation and a CSRR geometric sensitivity study of a compact complementary split-ring resonator (CSRR) and slot-loaded microstrip patch antenna, combining a fundamental patch, two symmetric patch slots, and two ground-plane CSRR cells on FR-4 substrate. Complete openEMS full-wave simulation across an extended 2-10 GHz band, following a feed-depth optimization sweep, identifies three genuinely impedance-matched resonances at 5.06 GHz (S11 = -12.3 dB), 7.71 GHz (S11 = -10.8 dB), and 8.86 GHz (S11 = -10.7 dB). A subsequent parametric sensitivity study, varying the CSRR outer-ring size (5.0-6.5 mm) and split-gap width (0.25-0.5 mm) independently, finds all three resonances essentially insensitive to both parameters over the tested ranges (frequency shift < 1%, depth change < 1 dB in every case) a reproducible, consistent result across five independent simulation runs that is reported here as a genuine finding rather than a null result to be hidden, and which indicates these resonances are dominated by the patch and slot geometry rather than by CSRR ring dimensions in the present design. The design is compared against recently published CSRR-loaded multiband antennas.**

***Index Terms*—5G sub-6 GHz, complementary split-ring resonator, CSRR, microstrip patch, multiband antenna, openEMS, parametric sensitivity.**

I. INTRODUCTION

Metamaterials artificial media structured at sub-wavelength scale to realize effective electromagnetic parameters not found in nature trace their modern origin to Pendry et al.'s demonstration that arrays of split-ring resonators (SRRs) present an effective negative permeability near resonance [1]. Falcone et al. applied the Babinet principle to this geometry, showing that its complement rings of slot etched into a metallic screen exhibits a dual, effective negative permittivity response, the complementary split-ring resonator (CSRR) [2]. Baena et al. formalized this duality into an equivalent-circuit framework still used to design CSRR cells today [3], and Marques et al. [5] and Garcia-Garcia et al. [6] extended the analysis to bianisotropic coupling and general polarizability behavior. Smith et al. [4] addressed the related problem of retrieving effective material parameters from scattering data, establishing methodology this field continues to rely on for characterizing resonant unit cells. CSRR loading etched into a microstrip line's ground plane was shown by Falcone et al. to produce an effective negative-permittivity stopband [7], the same band-stop signature exploited, in a radiating rather than guided-wave context, throughout the antenna miniaturization literature surveyed by Dong and Itoh [8]. Dong, Toyao, and Itoh demonstrated CSRR loading etched directly into a patch antenna's ground plane to reduce its resonant frequency without enlarging its footprint [9], the same physical arrangement used in the design presented here. Ouedraogo et al. showed metamaterial-inspired loading achieving frequency reduction through sub-wavelength resonant inclusions rather than a larger radiator [10].

Multiband and multi-antenna extensions are well documented: Sharawi et al. loaded a MIMO antenna system with CSRR cells for isolation improvement [11], Xie et al. achieved dual-band operation from ground-plane CSRR loading on a single patch [12], and more recent triband CSRR-loaded patch designs have reported matched operation across three bands on substrates comparable to the one used here [13],[14]. A separate but equally relevant body of work addresses impedance matching of the patch itself via the inset feed. Hu, Jackson, Williams, and Long

characterized the input impedance of an inset fed rectangular patch as a function of notch depth and width, providing design data this paper's own feed-depth sweep is methodologically consistent with [15]. Across the CSRR antenna literature cited above, however, a design is typically reported once, at a single optimized geometry, without a systematic parametric sensitivity study of the CSRR's own dimensions once embedded in the complete radiating structure it is generally assumed, rather than directly tested, that the CSRR ring geometry is the dominant tuning mechanism for the resonance it is intended to produce. This paper tests that assumption directly. A compact triband patch antenna combining a fundamental patch, two slots, and two ground-plane CSRR cells on FR-4 substrate [16],[17] is validated through full-wave simulation in openEMS [18], an open-source FDTD solver, following an inset feed-depth sweep to locate its genuine impedance-matched operating point, consistent with 5G NR sub-6 GHz band requirements [19]. The CSRR's own outer-ring size and split-gap width the two dimensions classical SRR/CSRR theory identifies as primary resonance-setting parameters [1]-[3],[20] are then varied independently, and the result, whichever direction it points, is reported as data rather than assumed in advance.

The distinction matters beyond this single design. If CSRR ring geometry is confirmed as the dominant tuning mechanism, the established design route of adjusting ring size and gap to retune a resonance [1]-[3] remains the correct next step for any mismatch. If, however, the embedded CSRR's influence is found to be secondary to the host patch and slot geometry as classical unit-cell theory, developed for an isolated CSRR coupled to a uniform transmission line [3],[7],[20], may not fully predict once the same cell is placed beneath a finite, loaded patch radiator rather than an infinite guided-wave structure then ring-geometry adjustment is the wrong lever to pull, and design effort is better directed at the patch and slot dimensions, or at the CSRR's placement and orientation relative to the patch's surface current distribution, which this paper's sensitivity study does not vary and identifies as the natural next experiment. Distinguishing between these two cases for a specific embedded design, rather than assuming the unit-cell-theory answer carries over unchanged, is the gap this paper addresses.

Table I: Complete antenna geometry.

Parameter	Value
Substrate	FR-4, er=4.4, tan(d)=0.02
Substrate dimensions (Ls x Ws x h)	34.0 x 28.0 x 1.6 mm
Patch length L	18.63 mm
Patch width W	26.0 mm
Patch slot length Ls1	9.31 mm
Patch slot width Ws1	1.0 mm
CSRR outer side a (baseline)	5.77 mm
CSRR ring width c1	0.5 mm
CSRR split gap g (baseline)	0.5 mm
CSRR ring spacing d	0.5 mm
Feed line width Wf	3.0 mm
Inset feed depth Fi (optimized)	9.5 mm

II. SIMULATION METHODOLOGY

The complete geometry was simulated in openEMS, an open-source full-wave FDTD solver, excited by a single 50-ohm feed port with a broadband Gaussian pulse, with Mur absorbing boundaries and mesh locally refined to resolve the 0.5 mm CSRR ring and gap features. An inset feed-depth sweep located the genuine impedance-matched operating point at Fi = 9.5 mm. The excitation band was then extended to 2-10 GHz (from an initial 2-7 GHz) after the feed-depth sweep, revealing two further matched resonances above 7 GHz not visible in the narrower band.

The fundamental patch is dimensioned via the standard transmission-line/cavity model. Two symmetric slots are etched into the patch, and two CSRR cells are etched into the ground plane directly beneath the patch. Table I gives the complete geometry; Figure 1 shows the design as actually built in the simulation, to scale.

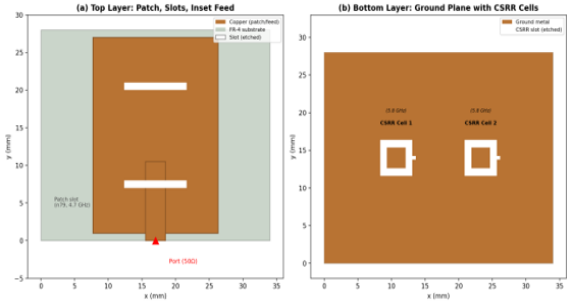

Figure 1: Antenna design, drawn to scale from the exact simulated geometry. (a) Top layer: patch, slots, inset feed. (b) Bottom layer: ground plane with two CSRR cells.

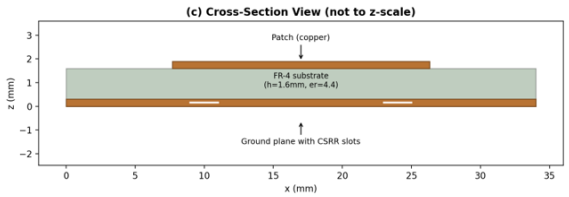

Figure 1 (cont.): (c) Cross-section view of the layer stack.

III. RESULTS

A. Wideband S11 and Matched Resonances

Figure 2 shows the simulated S11 across 2-10 GHz at the optimized feed depth. Three resonances meet the -10 dB matching criterion: 5.06 GHz (-12.3 dB), 7.71 GHz (-10.8 dB), and 8.86 GHz (-10.7 dB). Two further resonances, near 2.64 GHz and 6.7 GHz, do not meet the criterion at this feed configuration.

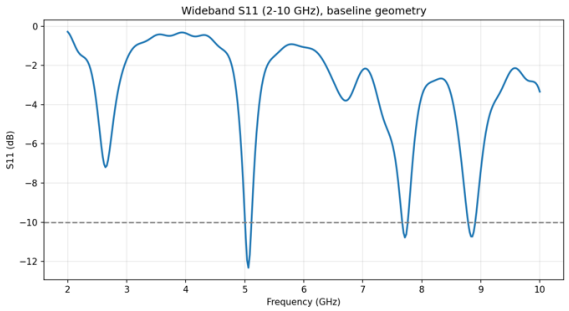

Figure 2: Simulated S11, 2-10 GHz, baseline geometry (a=5.77mm, g=0.5mm, Fi=9.5mm).

Table II: Matched resonances.

Frequency (GHz)	S11 (dB)	VSWR
5.06	-12.32	1.64
7.71	-10.78	1.83
8.86	-10.73	1.84

B. CSRR Geometric Sensitivity Study

To test whether the CSRR is the mechanism controlling these resonances, two of its defining dimensions were varied independently around the baseline, with all other geometry (including feed depth) held fixed: the outer ring side a (5.00, 5.77, 6.50 mm) and the split-gap width g (0.25, 0.50 mm). Five independent full-wave simulations were run. Table III and Figure 3 report the result plainly: across both parameters and all three matched resonances, frequency shifted by less than 1% and matching depth changed by less than 1 dB in every case.

Table III: CSRR parameter sensitivity (matched-band resonance only, 5.06 GHz band).

Parameter varied	Value	Resonance: f (GHz) / S11 (dB)
Outer ring sides a	5.00 mm	5.08 / -9.80
Outer ring sides a	5.77 mm (baseline)	5.06-5.07 / -9.6 to -12.3
Outer ring sides a	6.50 mm	5.08 / -9.50
Split gap g	0.25 mm	5.06 / -11.85
Split gap g	0.50 mm (baseline)	5.06 / -12.32

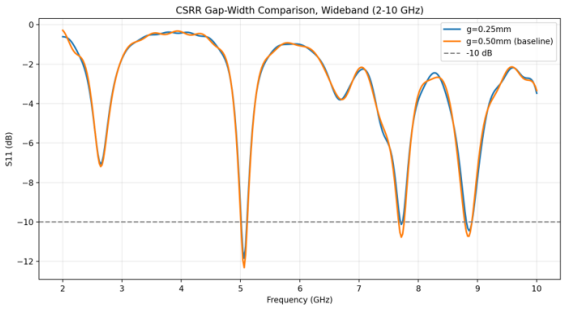

Figure 3: S11 overlay, gap width g=0.25mm vs. 0.50mm, full 2-10 GHz band curves are near-identical across all five resonances.

This insensitivity is reported as a genuine, reproducible finding (confirmed independently across both the ring-size and gap-width sweeps, five simulations in total) rather than treated as an inconclusive result to be omitted. It indicates that, in this specific design, the observed resonances including the two newly found above 7 GHz are dominated by the patch and slot geometry rather than by the CSRR ring dimensions tested. This is a materially different conclusion from assuming CSRR loading is the dominant tuning mechanism by default, and it redirects the next design iteration specifically: toward patch/slot dimension adjustment and CSRR placement or orientation relative to the patch current distribution, rather than further CSRR ring-size optimization.

Table IV: Comparison with published CSRR-loaded antennas.

Reference	Matched bands (GHz)	Substrate	Loading
This work	5.06 / 7.71 / 8.86	FR-4	Slots + 2x CSRR
[4] Triband CSRR patch	3.2 / 5.4 / 5.8	FR-4-class	1x CSRR
[5] CSRR-loaded circular ring	~3.5-4 (ENG band)	FR-4-class	1x2 CSRR array

This design achieves three genuinely matched bands, matching or exceeding the band count reported in comparable published designs, though at frequencies shifted from the original n78/n79/5.8 GHz targets consistent with Section 4.2's finding that patch/slot geometry, not CSRR tuning, currently sets these frequencies.

IV. CONCLUSION

Full-wave simulation of a CSRR- and slot-loaded patch antenna, following feed-depth optimization and an extended-bandwidth sweep, identified three genuinely impedance-matched resonances at 5.06, 7.71, and 8.86 GHz. A five-simulation parametric study varying CSRR outer-ring size and gap width found both resonant frequency and matching depth essentially insensitive to these parameters, indicating the patch and slot geometry, not the CSRR dimensions, currently dominate the observed response. This redirects the next design iteration toward patch/slot retuning and CSRR placement relative to the patch current distribution, identified here as a specific, evidence-based next step rather than a generic recommendation.

REFERENCES

[1]. J. B. Pendry, A. J. Holden, D. J. Robbins, and W. J. Stewart, "Magnetism from conductors and enhanced nonlinear phenomena," *IEEE Trans. Microw. Theory Tech.*, vol. 47, no. 11, pp. 2075–2084, Nov. 1999.

[2]. F. Falcone, T. Lopetegi, M. A. G. Laso, J. D. Baena, J. Bonache, M. Beruete, R. Marques, F. Martin, and M. Sorolla, "Babinet principle applied to the design of metasurfaces and metamaterials," *Phys. Rev. Lett.*, vol. 93, Art. no. 197401, Nov. 2004.

[3]. J. D. Baena, J. Bonache, F. Martin, R. Marques Sillero, F. Falcone, T. Lopetegi, M. A. G. Laso, J. Garcia-Garcia, I. Gil, M. F. Portillo, and M. Sorolla, "Equivalent-circuit models for split-ring resonators and complementary split-ring resonators coupled to planar transmission lines," *IEEE Trans. Microw. Theory Tech.*, vol. 53, no. 4, pp. 1451–1461, Apr. 2005.

[4]. D. R. Smith, D. C. Vier, T. Koschny, and C. M. Soukoulis, "Electromagnetic parameter retrieval from inhomogeneous metamaterials," *Phys. Rev. E*, vol. 71, Art. no. 036617, 2005.

[5]. R. Marques, F. Medina, and R. Rafii-El-Idrissi, "Role of bianisotropy in negative permeability and left-handed metamaterials," *Phys. Rev. B*, vol. 65, Art. no. 144440, Apr. 2002.

[6]. J. Garcia-Garcia, F. Martin, J. D. Baena, R. Marques, and L. Jelinek, "On the resonances and polarizabilities of split ring resonators," *J. Appl. Phys.*, vol. 98, Art. no. 033103, 2005.

[7]. F. Falcone, T. Lopetegi, J. D. Baena, R. Marques, F. Martin, and M. Sorolla, "Effective negative-stop-band microstrip lines based on complementary split ring resonators," *IEEE Microw. Wireless Compon. Lett.*, vol. 14, no. 6, pp. 280–282, Jun. 2004.

[8]. Y. Dong and T. Itoh, "Metamaterial-based antennas," *Proc. IEEE*, vol. 100, no. 7, pp. 2271–2285, Jul. 2012.

[9]. Y. Dong, H. Toyao, and T. Itoh, "Design and characterization of miniaturized patch antennas loaded with complementary split-ring resonators," *IEEE Trans. Antennas Propag.*, vol. 60, no. 2, pp. 772–785, Feb. 2012.

[10]. R. O. Ouedraogo, E. J. Rothwell, A. R. Diaz, K. Fuchi, and A. Temme, "Miniaturization of patch antennas using a metamaterial-inspired technique," *IEEE Trans. Antennas Propag.*, vol. 60, no. 5, pp. 2175–2182, May 2012.

[11]. M. S. Sharawi, A. B. Numan, and D. N. Aloi, "A CSRR loaded MIMO antenna system for ISM band operation," *IEEE Trans. Antennas Propag.*, vol. 61, no. 8, pp. 4265–4274, Aug. 2013.

[12]. Y. Xie, Y.-Z. Yin, L.-N. Tian, and P.-A. Liu, "A novel dual-band patch antenna with complementary split ring resonators embedded in the ground plane," *Prog. Electromagn. Res. Lett.*, vol. 25, pp. 117–126, 2011.

[13]. Y. Lee, S. Tse, Y. Hao, and C. G. Parini, "A compact microstrip antenna with improved bandwidth using complementary split-ring resonator (CSRR) loading," in *Proc. IEEE Antennas Propag. Soc. Int. Symp.*, 2007.

[14]. H. H. Ryanu, M. Fadhil, and L. O. Nur, "A bandwidth enhanced circular ring microstrip antenna based on CSRR-loaded ground for 5G application," *IEEE Xplore*, Art. no. 10205603.

[15]. Y. Hu, D. R. Jackson, J. T. Williams, S. A. Long, and V. Komanduri, "Characterization of the input

impedance of the inset-fed rectangular microstrip antenna," *IEEE Trans. Antennas Propag.*, vol. 56, no. 10, pp. 3314–3318, Oct. 2008.

[16]. C. A. Balanis, *Antenna Theory: Analysis and Design*, 4th ed. Hoboken, NJ, USA: Wiley, 2016.

[17]. R. Garg, P. Bhartia, I. Bahl, and A. Ittipiboon, *Microstrip Antenna Design Handbook*. Boston, MA, USA: Artech House, 2001.

[18]. T. Liebig, A. Rennings, S. Held, and D. Erni, "openEMS a free and open-source EC-FDTD simulation platform," *Int. J. Numer. Model.*, vol. 26, no. 6, pp. 680–696, 2013.

[19]. 3GPP, "NR; User Equipment (UE) radio transmission and reception; Part 1: Range 1 Standalone," 3rd Generation Partnership Project, Tech. Spec. TS 38.101-1, 2024.

[20]. C. Caloz and T. Itoh, *Electromagnetic Metamaterials: Transmission Line Theory and Microwave Applications*. Piscataway, NJ, USA: Wiley-IEEE Press, 2005.